

Conductance fluctuations in the localized regime

A. M. Somoza, J. Prior and M. Ortuno

Departamento de Física, Universidad de Murcia, Murcia 30.071, Spain

Abstract

We have studied numerically the fluctuations of the conductance, g , in two-dimensional, three-dimensional and four-dimensional disordered non-interacting systems. We have checked that the variance of $\ln g$ varies with the lateral sample size as $L^{2/5}$ in three-dimensional systems, and as a logarithm in four-dimensional systems. The precise knowledge of the dependence of this variance with system size allows us to test the single-parameter scaling hypothesis in three-dimensional systems. We have also calculated the third cumulant of the distribution of $\ln g$ in two- and three-dimensional systems, and have found that in both cases it diverges with the exponent of the variance times $3/2$, remaining relevant in the large size limit.

I. INTRODUCTION

The distribution function of the conductance of disordered systems is very well understood in the metallic regime, but poorly understood in the localized phase. According to the single-parameter scaling (SPS) hypothesis [1] the full conductance distribution function is governed by a single parameter. It is usual to choose the ratio of the system size L to the localization length ξ as the scaling parameter, but one could alternatively choose, for example, the average of the conductance.

The validity of the SPS hypothesis has been thoroughly checked in one-dimensional (1D) systems. In this case, it has been shown that, all the cumulants of $\ln g$ scale linearly with system size [2]. Thus, the distribution function of $\ln g$ approaches a Gaussian form for asymptotically long systems. In this limit, this distribution is fully characterized by two parameters, the mean $\langle \ln g \rangle$ and the variance of $\ln g$

$$\sigma^2 = \langle \ln^2 g \rangle - \langle \ln g \rangle^2 : \quad (1)$$

Both parameters are related to each other through the relation

$$\sigma^2 = L = 1 ; \quad (2)$$

which justify SPS in 1D systems. Here ξ is the localization length, defined in terms of the decay of the average of the logarithm of the conductance as a function of the length of the system L as

$$\xi = \lim_{L \rightarrow \infty} \frac{2L}{\langle \ln g \rangle} : \quad (3)$$

Eq. (2) was first derived within the so-called random phase hypothesis [3], and it has been proven to hold for most models. However, it is not verified in the band tails [4], in the center of the band [5, 6] or for very strong disorders [7].

The situation in higher dimensions is not as clear as in 1D systems. In those dimensions is far more difficult to do analytical calculations and numerical simulations have been limited until recently to small sample sizes. In the strong localization regime, $\ln g$ was claimed to be normally distributed and the variance was assumed to depend linearly on size in two-dimensional (2D) and three-dimensional (3D) systems [8, 9]. Recently, it has been pointed out that this distribution is not log normal [10, 11]. Slevin, A sado and Deych [12] studied the variance of the Liapunov exponent and checked the SPS hypothesis in 2D systems.

Nguyen et al. [13] proposed a model to account for quantum interference effects in the localized regime, where the tunneling amplitude between two sites was calculated considering only the shortest or forward-scattering paths. In the SPS regime the localization length must be much larger than the lattice constant, this means that contributions from other paths cannot be negligible. But, as the contribution of each path decay exponentially with its distance, we can expect that some properties of the conductance distribution (in particular the size dependence) should be dominated by the shortest paths. Medina and Kardar [14, 15] studied in detail the model. They computed numerically the probability distribution for tunneling and found that is approximately log normal, with its variance increasing with distance as $r^{2=3}$ for 2D systems. This is in contrast with the 1D case, where the variance grows linearly with distance, and with the implicit assumptions of some works on 2D systems.

For 2D systems, we found numerically that the variance behaves as [16]

$$\sigma^2 = A h \ln g_i + B \quad (4)$$

with the exponent equal to $2=3$. This is a general result that holds for the Anderson model and Nguyen et al. (NSS) model and for different geometries in 2D systems. The constants A and B are model or geometry dependent. The precise knowledge of the dependence of σ^2 with $h \ln g_i$ made much easier the numerical verification of the SPS hypothesis. We checked this hypothesis for the Anderson model [16]. As we will see, the NSS model does not verify the SPS hypothesis. From a numerical point of view it is more convenient to use $h \ln g_i$ than $L=$ as the scaling variable, since one does not have to calculate the localization length. It also facilitates a possible comparison with experiments.

The conductance distribution in the localized regime in 3D systems has been studied recently by Markos et al. [17]. They showed that this distribution is not log normal and tried to fit it with an analytical model [17]. The relationship between the different moments of the distribution has not been deeply considered. The applicability of the SPS hypothesis in the critical regime of the Anderson model has also been verified [18, 19].

Our goal in this paper is to find the dependence of the variance of $\ln g$ with its average for dimensions higher than two in the strongly localized regime. In particular, we will investigate if Eq. (4) is valid in these dimensions, with a dimension dependent exponent. We will also study the third central moment in 3D systems.

In the next section, we describe the two models we have used in our calculations. In

section 3, we present the results for the dependence of the variance of $\ln g$ in 3D systems. We will see that our results are consistent with the SPSS hypothesis. In section 4, we extend the previous results to four-dimensional (4D) systems and discuss the independent path approximation. In section 5, we show the behavior of the third cumulant, equal to the third central moment, and the skewness. We also comment about higher order cumulants. Finally, we discuss the results and extract some conclusions.

II. MODEL

We have studied numerically the Anderson model for 3D samples and NSS model for 3D and 4D samples. For the Anderson model, we consider cubic samples of size $L \times L \times L$ described by the standard Anderson Hamiltonian

$$H = \sum_i \epsilon_i a_i^\dagger a_i + t \sum_{i,j} a_j^\dagger a_i + \text{h.c.}; \quad (5)$$

where the operator a_i^\dagger (a_i) creates (destroys) an electron at site i of a cubic lattice and ϵ_i is the energy of this site chosen randomly between $(-W/2; W/2)$ with uniform probability. The double sum runs over nearest neighbors. The hopping matrix element t is taken equal to 1, which sets the energy scale, and the lattice constant equal to 1, setting the length scale. All calculations with the Anderson model are done at an energy equal to 0.01, to avoid the center of the band.

We have calculated the zero temperature conductance g from the Green functions. The conductance G is proportional to the transmission coefficient T between two semi-infinite leads attached at opposite sides of the sample

$$g = \frac{2e^2}{h} T \quad (6)$$

where the factor of 2 comes from spin. From now on, we will measure the conductance in units of $2e^2/h$. The transmission coefficient can be obtained from the Green function, which can be calculated propagating layer by layer with the recursive Green function method [20, 21]. This drastically reduced the computational effort. Instead of inverting an $L^3 \times L^3$ matrix, we just have to invert L times $L^2 \times L^2$ matrices. With the iterative method we can easily solve cubic samples with lateral dimension from $L = 8$ to 35. We have considered ranges of disorder W from 20 to 30. The number of different realizations of the disorder

employed is of 2000 for most samples. The leads serve to obtain the conductivity from the transmission formula in a way well controlled theoretically and close to the experimental situation. We have considered wide leads with the same section as the samples, which are represented by the same hamiltonian as the system, Eq. (5), but without diagonal disorder. We use cyclic periodic boundary conditions in the direction perpendicular to the leads.

We have also studied the NSS model [13] and Medina and Kardar [14, 15] in 3D cubic samples and 4D hypercubic samples. In this model, one considers an Anderson hamiltonian, Eq. (5), in which the diagonal disorder can only take two values $W=2$ and $W=-2$. One concentrates on the transmission amplitude between two points in opposite corners of the sample and assumes that the quantum trajectories joining these two points have to follow one of the (many) shortest possible paths. The transmission at zero energy is equal to [14]

$$T = \frac{2t}{W} J^2(l) ; \quad (7)$$

where the transmission amplitude $J(l)$ is given by the sum over all the directed or forward-scattering paths

$$J(l) = \sum_{\text{directed}} J ; \quad (8)$$

The contribution of each path, J , is the product of the signs of the disorder along the path and l is the length of the paths. The system size L is proportional to the path length l , with a proportionality constant of the order of unity. Considering only directed paths is well justified in the strongly localized regime, where the contribution of each trajectory is exponentially small in its length. The variance of $\ln g$ is entirely determined by $J^2(l)$ and so it depends on L , but not on W in this model. To quantify the magnitude of the fluctuations, it is convenient to do it in terms of the length L in the NSS model. $\ln g$ is, of course, proportional to L , but the constant of proportionality depends on the disorder W .

The assumption of directed paths facilitates the computational problem and makes feasible to handle system sizes much larger than with the Anderson hamiltonian. The sum over the directed path can be obtained propagating layer by layer the weight of the trajectories starting at the initial position and passing through a certain point [14]. In order to maximize interference effects, it is interesting to consider the initial and final sites at opposite corners of the sample. To simplify the programming complexity of the problem in 3D systems, we have considered a BCC lattice with the vector joining the two terminal points along the

direction $(1,0,0)$. In this way we can propagate layer by layer, with each layer being a piece of a square lattice. For 4D systems we consider an "hyper-BCC" lattice such that the layers that we handle are pieces of a simple cubic lattice. We have calculated 3D samples with path lengths up to $l = 400$ and 4D samples with l up to 130. We have averaged over 2×10^6 realizations of the disorder in 3D systems and over 6×10^6 realizations in 4D systems.

III. VARIANCE OF THREE-DIMENSIONAL SYSTEMS

The aim of this section is to find if an expression of the form (4) also holds for 3D systems with an exponent characteristic of this dimension. To verify this law and to determine numerically this exponent in 3D systems we first use NSS model and represent σ^2 versus L on a double-logarithmic scale. Once we have an estimate of the exponent, which in our case turn out to be $\alpha = 2.5$, it is more demanding to represent σ^2 as a function of L on linear scales. This is what we do in Fig. 1 for NSS model in 3D systems. Each dot corresponds to a different system size. We see that the data follow an excellent straight line and so we conclude that, at least in this model, the variance of $\ln g$ verify the law

$$\sigma^2 = A h \ln g L^{2.5} + B ; \quad (9)$$

where A and B are model and/or geometry dependent constants. We have taken into account that $h \ln g$ is proportional to L .

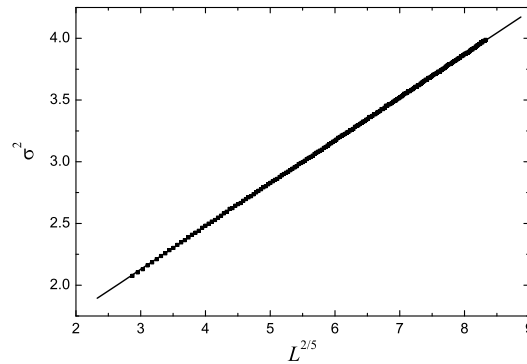


FIG. 1: σ^2 as a function of $L^{2.5}$ for NSS model in 3D systems.

NSS model is very convenient, because allows us to handle large sample size, but it involves certain approximations and does not satisfy the SP S hypothesis, since the variance

σ^2 does not depend on disorder, while $\ln g$ depends on both disorder and system size. Moreover, the conductivity of this model would correspond to a system with microscopically narrow leads attached to two points of the system, while in real systems wide leads of the order of the sample size are used. So, it is desirable to see if the previous results also apply to the Anderson model with wide leads. In Fig. 2 we plot σ^2 as a function of $\ln g$ for the Anderson model with wide leads in 3D systems for different values of the disorder $W = 20$ (squares), 25 (solid dots), 27 (up triangles) and 30 (down triangles). We see that the data again fit a straight line quite well. The straight line in Fig. 2 is a least square fit to the data and is given by

$$\sigma^2 = (5.71 \pm 0.12) \ln g - 6.0 \pm 0.3 \quad (10)$$

Care must be taken when extracting the power law behavior from a double logarithmic plot of σ^2 versus $\ln g$, due to the presence of the constant term, which in 3D systems is quite noticeable. Obviously, the previous behavior, Eq. (10), must break down since the behavior in the metallic part must be very different and, in any case, the variance cannot be negative. The critical point for the metal-insulator transition has been deeply studied and, for periodic boundary conditions, it corresponds to $\ln g = 1.280$ (in our units) for the largest sample size employed in Ref. 22 and to 1.329 for the largest size in Ref. 23. The variance at the critical point is in both works equal to 1.09. The crossing of our fitted behavior for the variance, Eq. (10), with this value of 1.09 gives us an estimate of the average of $\ln g$ at the critical point of 1.24 in very good agreement with the values obtained in Refs. 22, 23. We expect Eq. (10) to be pretty well satisfied in the entire localized regime down to the critical point.

A theoretical model for the conductance distribution in 3D systems in the localized regime was proposed by Markos et al. [17]. These authors calculated numerically the dependence of the variance of $\ln g$ with its average and argued that this was compatible with their analytical model. In the strongly localized regime, this model predicts a linear dependence ($\sigma^2 \propto \ln g$), in disagreement with our results, which expand a larger range of values of $\ln g$.

The data for the Anderson model in Fig. 2 for the different values of the disorder overlap within the error bars in a single line. The good overlap of the data is a strong support of the validity of the SPS hypothesis, since it shows that the variance σ^2 only depends on the

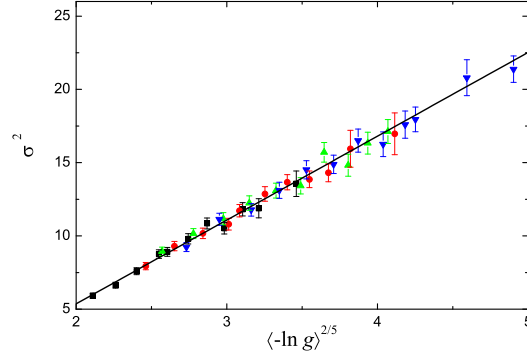


FIG. 2: (Color online) σ^2 versus $\langle \ln g \rangle^{2/5}$ for the Anderson model in 3D systems. Each symbol corresponds to a different disorder: 20 (squares), 25 (solid dots), 27 (up triangles) and 30 (down triangles).

mean of $\ln g$ and not on W and L separately.

The exponent that relates the variance of $\ln g$ and $\langle \ln g \rangle$ in Eq. (4) is 1 in 1D systems, $2=3$ in 2D systems and $2=5$ in 3D systems. These three results can be summarized in the following heuristic law

$$\sigma^2 = \frac{2}{2^{d-1} + 1}; \quad (11)$$

where d is the dimensionality of the system.

IV. VARIANCE OF FOUR-DIMENSIONAL SYSTEMS

An interesting question is to know if Eq. (4) also applies to 4D systems. It is quite difficult to check this with the Anderson model, but not so with NSS model. We have been able to calculate lateral sizes up to 120 and average over 2×10^6 samples. The results seem to indicate that the variance of $\ln g$ goes as the logarithm of L . In Fig. 3 we plot σ^2 as a function of L in a logarithmic scale. We note that the data can be fitted fairly well by a straight line. In the inset of Fig. 3 we represent the same data as in the main part of the figure as a function of $L^{2/9}$ on linear scales. The straight line is a linear least square fit of the data for large sizes only. The exponent $2=9$ is the one predicted by Eq. (11) for 4D systems. Other extrapolation schemes of the power law exponent to four dimensions will likely produce values larger than this one. It is easy to appreciate in the inset of Fig. 3 than

the logarithmic fit (main part of the figure) is better than this power law fit. A power law behaviour cannot be ruled out if finite size effects were relevant, although in 2D and 3D systems these effects are negligible.

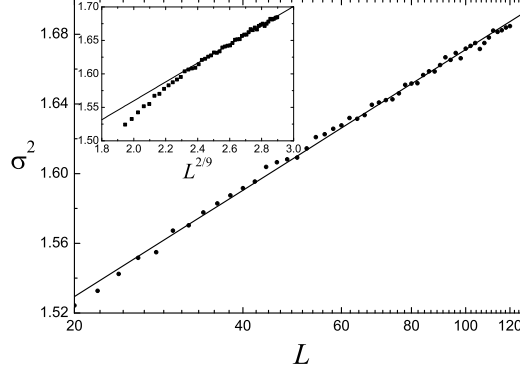


FIG. 3: σ^2 as a function of L in a logarithmic scale for NSS model in 4D systems. Inset: the same data as in the main part of the figure as a function of $L^{2/9}$.

In order to explain the results in 2D and 3D systems, one would have to take into account the correlations between the different trajectories ending in a given point. An approach has been developed along these lines for 2D systems [14]. These authors were interested in calculating $\langle J^{2n} \rangle$, where J is given by Eq. (8) (odd powers of J cancel by symmetry). They mapped approximately this problem to a quantum system of n interacting particles in one dimension less than the real dimension, $d^0 = d - 1$. The interaction between particles takes approximately into account the effect on intersections between different paths. As noted by Medina and Kardar, for dimension $d > 3$ ($d^0 > 2$ for the quantum system) there is a possible phase transition, depending on the amount of attraction. For large enough attraction then particles are bounded (intersections between paths are important), otherwise the attraction becomes asymptotically irrelevant and the behaviour is like free particles (intersections between paths are irrelevant). Obviously the expected relationship between mean and variance of $\ln g$ must change if we cross this phase transition. In the case that Eq. (11) could be applied also to 4D systems it should correspond to the region of bound states. The NSS model does not have free parameters to control the effect of intersections and it seems that for 4D systems we have already crossed the phase transition. It might be interesting to test Eq. (11) in the region of bound states, but this requires a new different

model.

In order to explain the results for 4D, we may assume that the intersections between paths are asymptotically irrelevant and apply the independent path approach [24]. In this approximation one assumes that the contributions J of the different paths in Eq. (8) are uncorrelated. Then the distribution of $J(L)$ tends to a gaussian with zero mean, by symmetry, and a variance proportional to the number of directed paths, which grows exponentially with L . The corresponding distribution of $\ln g$, which under these circumstances is the natural variable, presents a mean linearly dependent on L and a constant variance. Thus, this approximation predicts $\gamma = 0$. Our results for 4D systems agree with this prediction, although with logarithmic corrections. These might be due to deviations from the central limit and we think that they may persist at any finite dimension.

V. THIRD AND FOURTH CUMULANTS

We have previously shown that in 2D systems, unlike in 1D systems, the distribution of $\ln g$ does not tend to a gaussian in the strongly localized regime, since the skewness tends to a constant, different from zero, in the limit of $h |\ln g|$ going to infinity [10]. The skewness of $\ln g$ is defined as

$$S_k = \frac{h(\ln g - h \ln g)^3 i}{3=2}; \quad (12)$$

where the numerator is equal to the third cumulant or central moment γ_3 . The skewness tends to a finite constant if the third cumulant scales as $h |\ln g|^3 =^2$.

We analyse the behaviour of the third cumulant as a function of $h |\ln g|$ or L in 3D systems. In figure 4 we show this third cumulant for NSS model versus $L^{3=5}$. The exponent $3=5$ is the one for which the skewness takes to a finite value in 3D systems, given that the variance grows as $L^{2=5}$. As the data follow a straight line, we deduce that the distribution tends to a constant, non gaussian shape.

In the inset of figure 4 we plot the skewness of the distribution of $\ln g$ as a function of L for the same data as in the main part of the figure. The horizontal line is our estimate of the skewness in the macroscopic limit, equal to 0.3, obtained from the slope of the data in the main part of the figure. The continuous function is obtained from the linear fits in

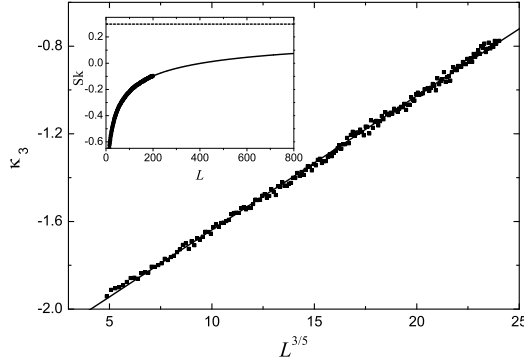


FIG .4: Third cumulant of $\ln g$ versus $L^{3/5}$ for the model of NSS in 3D systems. The corresponding skewness is represented in the inset.

figures (1) and (4):

$$Sk = \frac{A L^{3/5} + B}{(A^0 L^{2/5} + B^0)^{3/2}};$$

where $A; B; A^0$ and B^0 are the values obtained in the corresponding fits. We see that finite size effects are very large for the skewness due to the constant terms appearing in the dependence of the variance and (mainly) the third moment with $L^{2/5}$ and $L^{3/5}$, respectively.

The results for the third cumulant in the Anderson model in 3D systems are similar to those of NSS model. The results are consistent with Eq. (13), although the error bars are large. The skewness tends to a constant value. Our estimate of this value is roughly 0.7, slightly larger than the maximum value obtained in Ref. 17.

The theorem of Marcinkiewicz [25] shows that the cumulant generating function cannot be a polynomial of degree greater than 2, that is, either all but the first two cumulants vanish or there are an infinite number of nonvanishing cumulants. In the asymptotic limit the cumulants diverge in general, but we assume that there is a well defined distribution after an appropriate standardization procedure in terms of the variance. Then, Marcinkiewicz theorem imposes a strong condition on the asymptotic behavior of the cumulants. We are left with the following possible scenarios. The cumulant of order n , κ_n , for $n > 2$ grows as

$$\kappa_n / h \ln g i^{n-2} \quad (13)$$

where as before h is the exponent characterizing the variance, Eq. (4). In this case, the skewness and similar higher order quantities tend to constants different from zero. The

other possibility is that all the κ_n with $n > 2$ grow with an exponent smaller than $n=2$. Then the distribution of $\ln g$ tends to a gaussian. The third possibility, that the exponent characterizing κ_n is larger than $n=2$, would imply the use of this cumulant in the standardization procedure and the normalized variance would tend to zero. We assume that this is not possible and we are left with the first two scenarios: either all higher order moments grow like in Eq. (13) or the distribution tends to a gaussian.

We have seen that, unlike in 1D systems, 2D and 3D systems belong to the first scenario, since the skewness tends to a constant, and so we expect that all higher moments verify Eq. (13). We have verified this result for the fourth cumulant for the NSS model in 2D and 3D systems. In Fig. 5 we represent the fourth cumulant of the distribution of $\ln g$ as a function of $L^{4/3}$ for the model of NSS in 2D systems. We note that, as expected, the data fit a straight line fairly well.

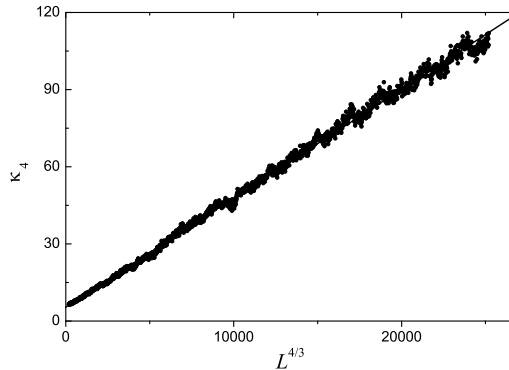


FIG. 5: Fourth cumulant of the distribution of $\ln g$ versus $L^{4/3}$ for the model of NSS in 2D systems.

VI. DISCUSSION AND CONCLUSIONS

In Table 1 we summarize the results for the exponent with which the different cumulants scale with $\ln g$ as a function of the dimensionality of the system. The second column corresponds to the variance, the third and the fourth columns to the third and fourth cumulants, respectively. The last column is our prediction for the n -th cumulant taking into account our results for the variance and the theorem of Marcinkiewicz. The exponent for

TABLE I: Exponents relating the cumulants with $\ln g_i$ for dimensions 1, 2, 3 and 4.

Dimension	2	3	4	n
1	1	1	1	1
2	2/3	1	4=3 ^a	n=3
3	2/5	3=5 ^b	?	n=5
4	0			

^aExponent obtained with the NSS model only.

^bExponent obtained with the NSS model and compatible with the Anderson model.

the fourth cumulant in 2D systems has only been obtained with the NSS model. The law for the third cumulant in 3D systems has been checked for the Anderson and the NSS models. The results for the NSS model are conclusive, while the results for the Anderson model are compatible, but not conclusive with the corresponding exponent.

In 1D systems, we know that all cumulants are proportional to L and we are in the second scenario, where only the first two cumulants are relevant for large sizes. In 2D and 3D systems, we are in the first scenario and furthermore there is one and only one cumulant (beside the mean) proportional to L . This cumulant is the third one in 2D systems and must be the fifth in 3D systems. The exponent of the variance (and of all cumulants) is determined from the order of this cumulant.

We have shown that the variance of $\ln g$ grows as $\ln g_i^{2=5}$ in 3D disordered non-interacting systems for the Anderson and NSS models. In the Anderson model, we have checked that the SPSS hypothesis is verified for energies in the band. In 4D systems, this variance goes as $\ln L$ in the NSS model. In dimensions higher than one, the distribution of $\ln g$ does not tend to a gaussian. So, higher order cumulants are relevant.

We have shown that the variance of $\ln g$ for dimensions higher than 1 grows more slowly than linear with system size. Specially the exponents $\alpha = 2=3$ in 2D systems and $\alpha = 2=5$ in 3D systems can be checked experimentally. We consider that a proper theoretical explanation of these two values is also an important challenge.

Acknowledgments

The authors would like to acknowledge financial support from the Spanish DGI, project number BFM 2003{04731 and a grant (JP).

-
- [1] E. Abrahams, P.W. Anderson, D.C. Liocciardello and T.V. Ramakrishnan, Phys. Rev. Lett. 42, 673 (1979).
 - [2] P.J. Roberts, J. Phys.: Condens. Matter 4, 7795 (1992).
 - [3] P.W. Anderson, D.J. Thouless, E. Abrahams, D.S. Fisher, Phys. Rev. B 22, 3519 (1980).
 - [4] L.I. Deych, A.A. Lisyansky and B.L. Altshuler, Phys. Rev. B 64, 224202 (2001).
 - [5] L.I. Deych, M.V. Entinzhuk, A.A. Lisyansky and B.L. Altshuler, Phys. Rev. Lett. 91, 096601 (2003).
 - [6] H. Schomerus and M. Titov, Phys. Rev. B 67, 100201(R) (2003).
 - [7] K.M. Slevin and J.B. Pendry, J. Phys.: Condens. Matter 2, 2821 (1990).
 - [8] K. Chase and A. Mackinnon, J. Phys. C 20, 6189 (1987).
 - [9] B. Kramer, A. Kawabata and M. Schreiber, Phil. Mag. B 65, 595 (1992).
 - [10] J. Prior, A.M. Somosa and M. Ortuño, Phys. Stat. Solidi (b), (2005).
 - [11] K.A. Muttalib, P. Markos and P. Wole, Phys. Rev. B 72, 125317 (2005).
 - [12] K. Slevin, Y. Asada and L.I. Deych, Phys. Rev. B 70, 054201 (2004).
 - [13] V.L. Nguyen, B.Z. Spivak and B.I. Shklovskii, Pis'ma Zh. Eksp. Teor. Fiz. 41, 35 (1985) [JETP Lett. 41, 42 (1985)]; Zh. Eksp. Teor. Fiz. 89, 11 (1985) [Sov. Phys. JETP 62, 1021 (1985)].
 - [14] E. Medina and M. Kardar, Phys. Rev. B 46, 9984 (1992).
 - [15] E. Medina, M. Kardar, Y. Shapir and X.R. Wang, Phys. Rev. Lett. 62, 941 (1989).
 - [16] J. Prior, A.M. Somosa and M. Ortuño, Phys. Rev. B 72, 024206 (2005).
 - [17] P. Markos, K.A. Muttalib, P. Wole and J.R. Klauder, Europhys. Letters 68, 867 (2004).
 - [18] K. Slevin, P. Markos and T. Ohtsuki, Phys. Rev. Lett. 86, 3594 (2001).
 - [19] K. Slevin, P. Markos and T. Ohtsuki, Phys. Rev. B 67, 155106 (2003).
 - [20] A. Mackinnon, Z. Phys. B 59, 385 (1985).
 - [21] J.A. Verges, Comput. Phys. Commun. 118, 71 (1999).

- [22] C. M. Soukoulis, X. Wang, Q. Li and M. M. Sigalas, Phys. Rev. Lett. 82, 668 (1999).
- [23] D. Braun, E. Hofstetter, G. Montambaux and A. Mackinnon, Phys. Rev. B 64, 155107 (2001).
- [24] O. Entin-Wohlman, C. Hertzstein and Y. Imry, Phys. Rev. B 34, 921 (1986); O. Entin-Wohlman, Y. Imry and U. Sivan, Phys. Rev. B 40, 8342 (1988).
- [25] J. Marcinkiewicz, Math. Z. 44, 612 (1939); G. W. Gardiner, Handbook of Stochastic Methods, 2nd ed. (Springer-Verlag, Berlin, 1985).